Calcitonin Gene-Related Peptide Influences Bone-Tendon Interface Healing Through Osteogenesis

Investigation in a Rabbit Partial Patellectomy Model

Huabin Chen,*[†] MD, Hongbin Lu,*[†] MD, PhD, Jianjun Huang,[‡] MM, Zhanwen Wang,*[†] MD, Yang Chen,*[†] MD, and Tao Zhang,*[†§] MD, PhD
Investigation performed at Xiangya Hospital, Central South University, Changsha, Hunan, People's Republic of China

Background: Calcitonin gene-related peptide (CGRP), which has been shown to play an important role in osteogenesis during fracture repair, is also widely distributed throughout the tendon and ligament. Few studies have focused on the role of CGRP in repair of the bone-tendon interface (BTI).

Purpose: To explore the effect of CGRP expression on BTI healing in a rabbit partial patellectomy model.

Study Design: Controlled laboratory study.

Methods: A total of 60 mature rabbits were subjected to a partial patellectomy and then randomly assigned to CGRP, CGRP-antagonist, and control groups. In the CGRP-antagonist group, the CGRP receptor antagonist BIBN4096BS was administered to block CGRP receptors. The patella–patellar tendon complex was harvested at 8 and 16 weeks postoperatively and subjected to radiographic, microlaser Raman spectroscopy, histologic, and biomechanical evaluation.

Results: Radiographic data showed that local CGRP expression improved the growth parameters of newly formed bone, including area and volumetric bone mineral density ($P < .05$ for both). Raman spectroscopy revealed that the relative bone mineral composition increased in the CGRP group compared with in the control group and the CGRP-antagonist group ($P < .05$ for both). Histologic testing revealed that the CGRP group demonstrated better integration, characterized by well-developed trabecular bone expansion from the residual patella and marrow cavity formation, at the 8- and 16-week time points. Mechanical testing demonstrated that the failure load, ultimate strength, and stiffness in the CGRP group were significantly higher than those in the control group ($P < .05$ for all), whereas these parameters in the CGRP-antagonist group were significantly lower compared with those in the control group at 16 weeks after surgery ($P < .05$ for all).

Conclusion: Increasing the local concentration of CGRP in the early stages of BTI healing enhanced osteogenesis in a rabbit partial patellectomy model and promoted healing of the BTI injury, whereas treatment using a CGRP antagonist had the opposite effect. However, exogenous CGRP expression did not induce novel bone remolding.

Clinical Relevance: CGRP may have potential as a new therapy for BTI injuries or may be added to postoperative regimens to facilitate healing.

Keywords: CGRP; CGRP receptor antagonist; bone tendon interface; osteogenesis; partial patellectomy

In sports medicine and orthopaedics, injury to the bone-tendon interface (BTI) is as common as rotator cuff tears and anterior cruciate ligament injuries. Owing to the composition of the BTI, which comprises both bone and tendon tissues, repair is difficult, and the failure rate is high.[2,6] In previous studies, researchers from our institution showed that the area,

length, and mineralization of newly formed bone in the BTI were closely related to healing quality.[10,17] In a rabbit partial patellectomy model, the location of failure in the operative samples was almost always at the initial osteotomy site between the newly formed bone and the residual patella.[19,33] This means that finding novel methods to facilitate high-quality osteogenesis at the BTI might be a critical factor in improving clinical outcomes for these injuries.

Existing data show that neural pathways, via their regulation of the systemic and local microenvironment, may

play an important role in the repair of bone and tendon injuries.[1,23] The sensory nerves are distributed widely in different bone and tendon tissues, including the rotator cuff[84] and patellar tendon,[5] and seem to act principally in the healing process via the release of neuropeptides.[7] Calcitonin gene-related peptide (CGRP) is considered one of the most important osteoanabolic neuropeptides[32,36] and is produced by both central and peripheral neurons. CGRP has been recognized as a neurotransmitter regulating bone formation in fracture healing.[3,12,15] However, the role of CGRP signaling in BTI injuries remains elusive.

A previous study using a rabbit model of mandibular bone defects showed that CGRP expression increased over a period of 14 days after injury, at which point it reached its maximum.[16] Interestingly, in a previous rabbit BTI injury model, the time frame of 2 weeks after partial patellectomy coincided with the transition from the inflammatory stage to new bone regeneration.[18] The purpose of the current study was to investigate the possible effects of CGRP expression on BTI healing. An established rabbit partial patellectomy model[10] was used, and injury remodeling was evaluated using histologic testing, microlaser Raman spectroscopy (MLRS), radiography, and biomechanical testing. We hypothesized that CGRP would enhance BTI healing by promoting osteogenesis.

METHODS

A total of 60 mature male New Zealand White rabbits (weight, 3.0-3.5 kg) were used to establish a BTI injury model and were randomly assigned to 1 of 3 groups: the CGPR group (n = 20), the CGRP-antagonist group (n = 20), and the control group (n = 20). Rabbits were sacrificed at 8 and 16 weeks after surgery, and tissues were collected for histologic and MLRS examination (5 rabbits per group per time point) and radiographic and biomechanical testing (5 rabbits per group per time point). This study protocol was approved by our institution.

Preparation of Fibrin Sealant Carriers

Fibrinogen and thrombin solutions (Sigma-Aldrich) were prepared according to the manufacturer's protocol. CGRP (Bioss Biotechnology) and BIBN4096BS (a CGRP-receptor antagonist; MedChemExpress) were added to the thrombin solution, and 200 μL of fibrinogen and 40 μL of thrombin solution were mixed to create the fibrin sealant. The final concentrations of CGRP and BIBN4096BS were 6.0 mg/L and 1.5 mg/L, respectively, in line with the concentrations used in other studies.[4,29,36] The control sealant was not supplemented using any additional compounds. The in vitro release dynamics for CGRP and the CGRP antagonist (BIBN4096BS) are described in Appendix Table A1.

Animal Surgery and Treatment

A partial patellectomy was performed on the left hind limbs of experimental animals as described previously.[33] After anesthetization using pentobarbital (0.8 mL/kg, intravenously; Sigma), the left knee of the rabbit was shaved, and the patella was exposed via an anterolateral skin incision. Transverse osteotomy was performed between the distal one-third and proximal two-thirds of the patella using a Synthes oscillating saw (Figure 1A). The distal one-third of the patella was discarded along with the fibrocartilage zone, and the proximal patella was sutured to the patellar tendon using 2 predrilled tunnels and absorbable sutures (No. 3-0 PDS II; Ethicon). Meanwhile, the fibrin sealant (control group), CGRP-supplemented fibrin sealant (CGRP group), or BIBN4096BS-supplemented fibrin sealant (CGRP-antagonist group) was secured to the surface of the interface of the patellar tendon and the remaining patella (Figure 1, B and C), and a figure-of-8 tension band wire (diameter, 0.4 mm) was wrapped around the patella to prevent the patella–patellar tendon (PPT) repair from overstretching (Figure 1D). After the surgical incision was closed, the damaged knee was immobilized in the resting position using a long cast for 4 weeks, with an open window for subsequent therapy. Tramadol (25 mg/L) was administered via the animals' drinking water for 7 days, and no animals experienced accidental death during the experimental process.

Sample Preparation

Animals were euthanized using an overdose of sodium pentobarbital at 8 or 16 weeks postoperatively. The bilateral PPT complex was harvested, wrapped using saline gauze, and stored at –20°C for radiographic and biomechanical testing.

For the histologic and MLRS analyses, samples were prepared and cut from the midsagittal plane using a sliding microtome (SM2500S; Leica) fitted with a tungsten carbide blade (Delaware Diamond Knives). One-half of each sample was stored at –20°C for MLRS, and the other half, used in the histologic evaluations, was fixed in 10% buffered formalin for 24 hours and then decalcified in EDTA for 3 weeks.
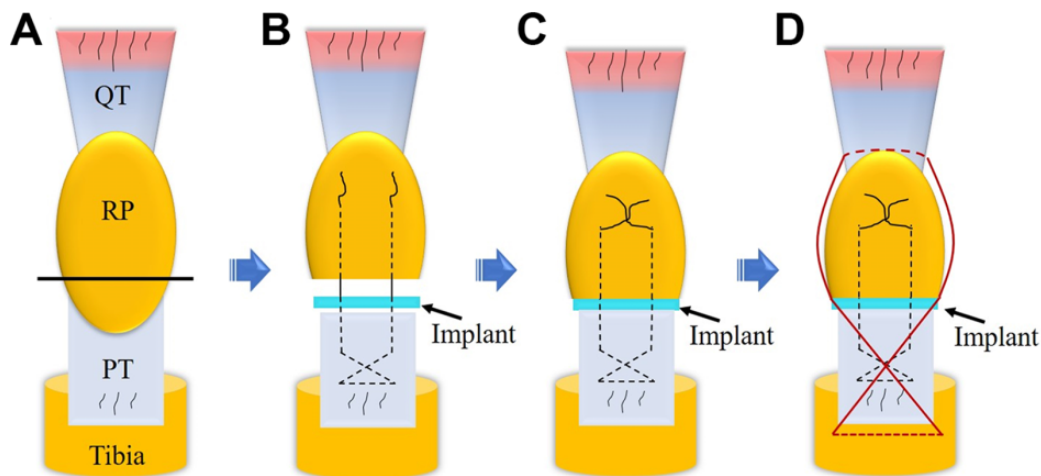
Figure 1. Illustration showing the rabbit partial patellectomy and implantation of the fibrin sealant (control group), CGRP-supplemented fibrin sealant (CGRP group), or BIBN4096BS-supplemented fibrin sealant (CGRP-antagonist group). (A) Transverse osteotomy was performed between the distal one-third and proximal two-thirds of the patella. (B, C) The remaining patella (RP), the implant, and the patellar tendon (PT) were sutured using No. 3-0 PDS IIsutures (Ethicon). (D) A figure-of-8 tension band wire was wrapped around the patella to prevent the patella–patella tendon repair from overstretching. CGRP, calcitonin gene-related peptide; QT, quadriceps tendon.

Radiographic Measurements

High-resolution anteroposterior radiographs of the PPT complex were obtained using 3 seconds of exposure time and a 60-kVp tube voltage. The distance of the source object was set to 40 cm, and after the radiographs were digitized using the Metamorph image analysis system (Universal Imaging Corp), the area of newly formed bone was measured as described in previous studies.[9,21]

Volumetric bone mineral density (BMD) of the new bone at the BTI was evaluated using peripheral quantitative computed tomography (pQCT; Scanco). The specimens were scanned at a spatial resolution of 0.3 mm and a CT slice thickness of 1 mm. An obvious change in volumetric BMD in continuous slices was predicated to be visible at the boundary between the new bone and the residual patella.[17]

Microlaser Raman Spectroscopy Analysis

MLRS is a method used to analyze the chemical composition of bone and other tissues. Scanning MLRS was performed at the Raman Spectroscopy Laboratory in the Powder Metallurgy Research Institute of Central South University (LabRAM Aramis; HORIBA Jobin Yvon). Samples were placed on a glass slide with the sagittal plane facing up, and the parameters were set as follows: Nd:YAG laser excitation, 532 nm; filter, 0.6; slit, 100 μm; grating, 1200; and exposure time, 5 seconds. The scanning spectrum ranged from 500 to 3500 Δcm^{-1}. The original Raman spectra were obtained and preprocessed to remove cosmic spikes and correct the fluorescence background. After preprocessing, information about the various components of the new bone was extracted. Generally, Raman spectroscopy is used to identify the mineral and matrix bands and ratios of band heights or band areas.[22] The phosphate υ1 band height

(960 cm^{-1}) was used as a surrogate for mineral content, and we evaluated the relative mineral content of the new bone by comparing this with the mineral content of the residual patella (band height at 960 cm^{-1}). The newly formed bone started from the point where the band height (960 cm^{-1}) changed suddenly.

Histologic Evaluation

After decalcification, the samples were embedded in paraffin, and the midsagittal sections (7 μm) were cut using a microtome. The slides were stained using hematoxylin and eosin (H&E) as previously described and were used for the descriptive analysis of the new bone.

Mechanical Testing

After pQCT scanning, PPT complexes were exposed to mechanical testing. A Hounsfield testing machine (H25k-S; Hounsfield Test Equipment) with a 2-kN load cell was used for all of these analyses.[33] After removal of the suture materials and the tension band, the PPT complexes were fixed on a custom clamp along the physiologic load axis. The width and thickness at the site of the transverse osteotomy were measured using a fine caliper under a constant 5-N tensile load. The cross-sectional area (CSA) of the repaired BTI was calculated. Then, the PPT complex was mounted on a custom-made tensile testing jig consisting of an upper clamp fastening the patella to the distal quadriceps and a lower clamp gripping the proximal tibia (Appendix Figure A1). The failure load of the PPT complex was then evaluated at a rate of 20 mm/min, and the stiffness was calculated using the linear portion of this curve. The ultimate strength values were determined using the failure load and CSA.
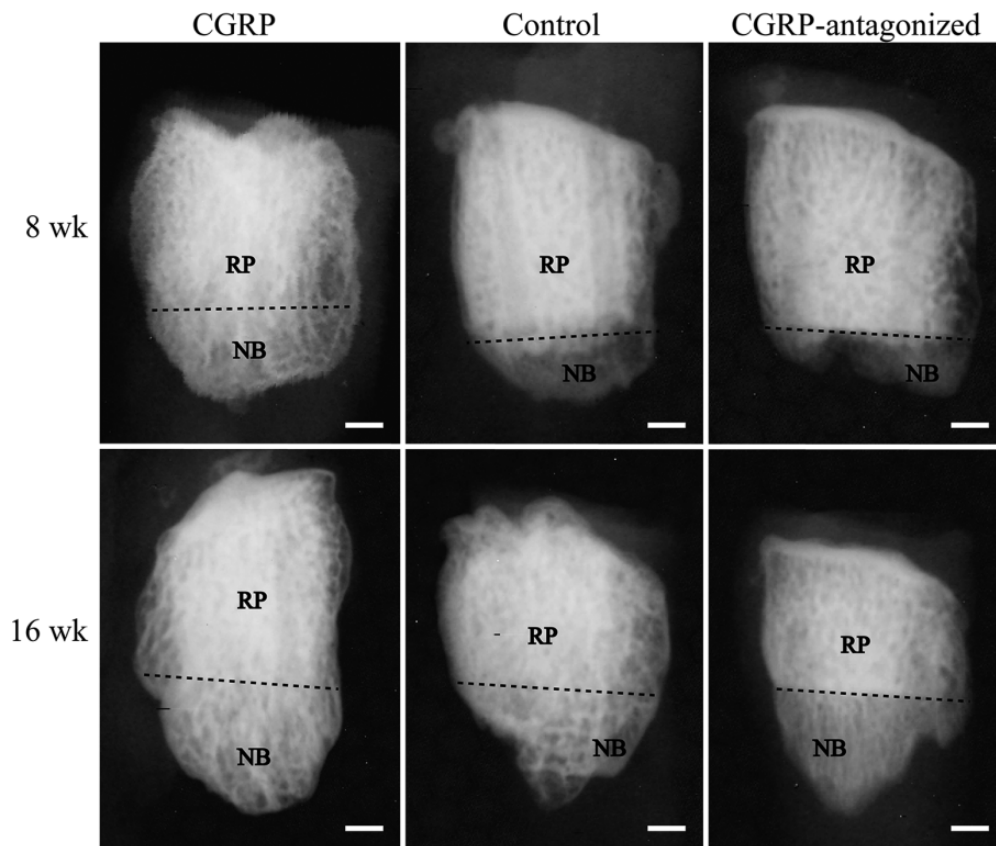
Figure 2. The newly formed bone, evaluated using anteroposterior radiographs, can be seen at the healing interface in each group at postoperative weeks 8 and 16. The new bone area increased between week 8 and week 16 in all 3 groups. The CGRP group produced more new bone at each time point compared with the control group, whereas the CGRP-antagonist group showed less new bone. The scale bars represent 1000 μm in all images. The dotted line represents the initial osteotomy site. CGRP, calcitonin gene-related peptide; NB, newly formed bone; RP, remaining patella.

Statistical Analysis

All quantitative data are reported as mean ± standard deviation and were evaluated for statistical significance using 2-way analysis of variance and the Bonferroni post hoc test. Statistical significance was set at $P < .05$. The power of the test was estimated using the multiple comparisons method proposed by O'Brien and Muller.[24] The power estimation was based on the F distribution using the noncentral parameter $N\dot{c}V/\sigma^2$ and degree of freedom $G - 1$ and $N - G$, respectively. We used the SAS macro program (SAS Institute Inc.) to perform these estimations.

According to the estimation, 5 rabbits from each group per time point was sufficient for analysis.

RESULTS

New Bone Mineralization

Area of New Bone. New bone was shown to extend from the proximal patella and was obvious at both 8 and 16 weeks postoperatively. This growth was shown to be significant in all groups, and the area of new bone growth enlarged over time in all 3 groups. The CGRP group demonstrated an increased production of new bone growth compared with the control group at both 8 weeks ($P < .01$) and 16 weeks ($P < .01$) postoperatively. This growth was significantly decreased at week 8 ($P < .05$) but not week 16 ($P > .05$) in the CGRP-antagonist group (Figure 2 and Table 1).

BMD of Newly Formed Bone Detected Using pQCT. The volumetric BMD of the newly formed bone in the CGRP group was significantly higher than that of the control group at week 8 ($P < .001$) but not at week 16 ($P > .05$). The BMD values for the CGRP-antagonist group (blocking CGRP receptors) were significantly lower than those of the control group at week 16 ($P < .001$) but not at week 8 ($P > .05$). When comparing the CGRP and CGRP-antagonist groups, we noted that the BMD of the new bone was lower when the CGRP receptors were blocked ($P < .001$ for both) at both 8 and 16 weeks (Table 1).

The area and BMD results suggest that CGRP may enhance osteogenesis around the PPT healing interface at early time points after partial patellectomy. This was confirmed by the fact that when the CGRP receptors were blocked using the BIBN4096BS inhibitor, bone regeneration decreased.

TABLE 1
Area and BMD of the Newly Formed Bone[a]

	8 Weeks Postoperatively			16 Weeks Postoperatively		
	CGRP	Control	CGRP Antagonist	CGRP	Control	CGRP Antagonist
Area, mm^2	7.82 ± 1.05^b	4.87 ± 0.85^c	$3.05 \pm 0.59^{b,c}$	10.31 ± 1.28^b	7.20 ± 1.44^c	6.43 ± 1.12^c
BMD, g/cm^3	1.27 ± 0.37^b	0.78 ± 0.15^c	0.67 ± 0.12^c	1.09 ± 0.18	0.85 ± 0.20	$0.31 \pm 0.16^{b,c}$

[a]Data are reported as mean ± SD. BMD, bone mineral density; CGRP, calcitonin gene-related peptide.
[b]Statistically significant difference compared with the control group at the same time point ($P < .05$).
[c]Statistically significant difference compared with the CGRP group at the same time point ($P < .05$).
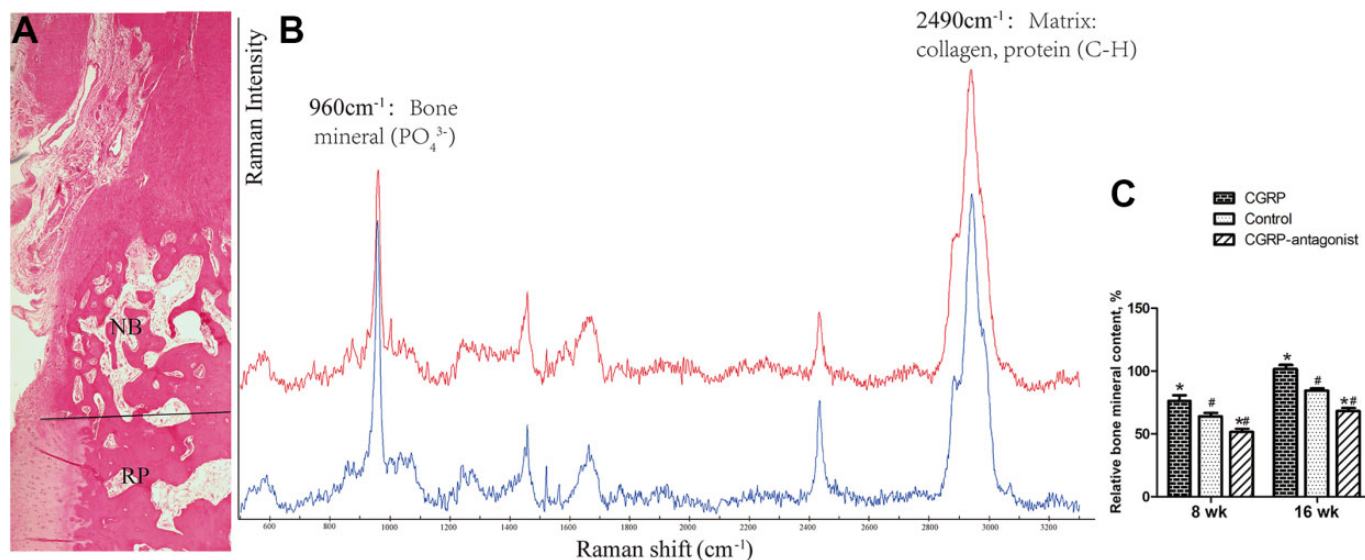

Figure 3. Raman spectroscopy detects bone tissues, including newly formed bone and the residual patella. (A) Midsagittal hematoxylin and eosin–stained micrographs show the areas of new bone (NB) and residual patella (RP). (B) Representative Raman spectrum of the NB (red curve) and RP (blue curve) in the rabbit patella–patellar tendon complexes. The ratios of the intensity of the 960 cm^{-1} peak in the NB and RP were used to calculate the relative bone mineral content (BMC) of the new bone tissue. (C) Statistical analysis of the relative BMC values for the newly formed bone in all 3 groups; n = 5 for each group per time point. *Statistically significant difference compared with the control group at the same time point ($P < .05$). #Statistically significant difference compared with the calcitonin gene-related peptide (CGRP) group at the same time point ($P < .05$). C-H, carbon-hydrogen bond.

Relative New Bone Mineral Content. MLRS measurements were performed on the rabbit PPT complex, and this analysis revealed a peak in the bone mineral band at 960 cm^{-1} (PO$_4^{3-}$) and several peaks at 2490 cm^{-1}, consistent with various proteins including collagen (carbon-hydrogen bond [CH]). The intensity of the residual patellar bone mineral signal (band at 960 cm^{-1}) was higher than that of newly formed bone (Figure 3, A and B). However, we could not guarantee that the scanning conditions were identical for all specimens, and for this reason, we reported the relative value of the new bone content compared with the residual patellar compositions. Relative bone mineral content (BMC) increased between week 8 and week 16 in all 3 groups. When we compared the 2 treatment groups versus the control group, we noted that the CGRP group had a higher relative BMC value (week 8: 76.20 ± 10.15 vs 63.96 ± 6.20, $P < .05$; week 16: 101.62 ± 7.23 vs 84.44 ± 4.01,

$P < .01$) and the CGRP-antagonist group had a significantly lower BMC value (week 8: 51.52 ± 5.79 vs 63.96 ± 6.20, $P < .05$; week 16: 64.18 ± 8.55 vs 84.44 ± 4.01, $P < .01$) than did the control group at weeks 8 and 16 (Figure 3C).

Histologic Results

The H&E-stained decalcified sections showed increasing new bone outgrowth over time, and these outgrowths started from the remaining patella in all 3 groups after partial patellectomy. At week 8, there was more woven bone in the CGRP group than in the other groups, and there seemed to be a fibrocartilaginous junction at the healing interface in the CGRP group. However, the lack of bone marrow cavities and lamellar bone formation suggested that the maturity of this newly formed bone was similar to that of the control group. In the CGRP-antagonist group,
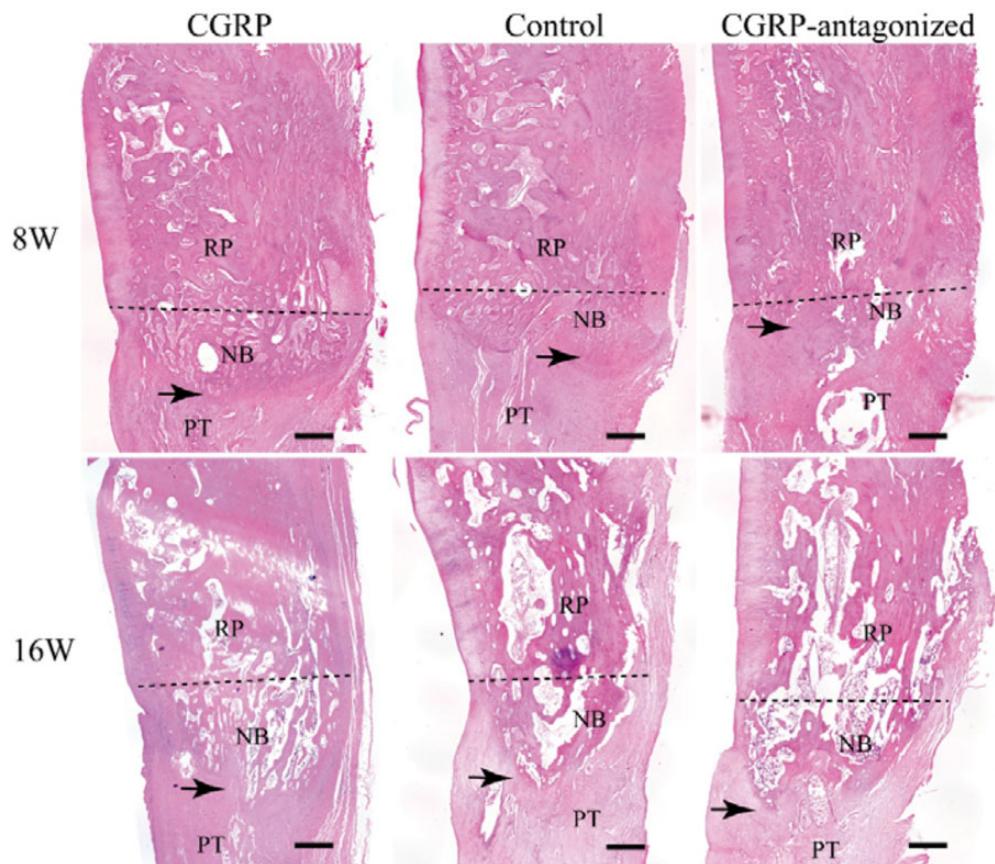
Figure 4. Representative midsagittal sections of the patella–patellar tendon interface of the CGRP-treated, control, and CGRP-antagonist groups at postoperative weeks 8 and 16. The black dotted line indicates the osteotomy site; the black arrow points to the regenerated fibrocartilage layer. Hematoxylin and eosin staining, n = 5 for each group per time point. Scale bar = 1000 μm. CGRP, calcitonin gene-related peptide; NB, newly formed bone; PT, patellar tendon; RP, remaining patella.

TABLE 2
Cross-Sectional Area and Biomechanical Properties of the Patella–Patellar Tendon Complexes[a]

	8 Weeks Postoperatively			16 Weeks Postoperatively		
	CGRP	Control	CGRP Antagonist	CGRP	Control	CGRP Antagonist
CSA, mm^2	50.22 ± 5.21^b	41.30 ± 6.23^c	35.25 ± 5.71^c	36.04 ± 6.09	43.32 ± 4.69	44.48 ± 3.17^c
Load to failure, N	183.00 ± 25.40	136.38 ± 21.22	107.22 ± 26.36^c	329.08 ± 39.18^b	249.00 ± 34.03^c	$184.94 \pm 36.01^{b,c}$
Ultimate strength, MPa	3.45 ± 0.38	3.32 ± 0.22	2.56 ± 0.08^c	7.68 ± 1.17^b	5.27 ± 0.69^c	$3.70 \pm 0.05^{b,c}$
Stiffness, N/mm	51.56 ± 3.22^b	43.64 ± 5.08^c	36.25 ± 4.05^c	67.68 ± 5.70^b	59.52 ± 4.18^c	$48.83 \pm 6.70^{b,c}$

[a]Data are reported as mean ± SD. CGRP, calcitonin gene-related peptide; CSA, cross-sectional area.
[b]Statistically significant difference compared with the control group at the same time point ($P < .05$).
[c]Statistically significant difference compared with the CGRP group at the same time point ($P < .05$).

the osteotomy surface between the newly formed bone and the original patella was still distinct at week 8 (Figure 4). At week 16, the healing and remodeling at the BTI were almost complete, characterized by trabecular bone, bone marrow cavities, and a nearly mature fibrocartilage layer. The CGRP group displayed better developed lamellar bone and had more new bone than did the other groups. Although the CGRP-antagonist group possessed plenty of large bone marrow cavities, there was less lamellar bone,

and the fibrocartilage zone was not as robust as that of the CGRP and control groups (Figure 4).

Biomechanical Testing

The results of the biomechanical testing are summarized in Table 2. Although scar tissue was formed and was shown to connect the tendon and patella in all 3 groups, the healing process and the biomechanical properties of the PPT

complexes were different among the 3 groups. At postoperative week 8, the CSA for the CGRP group was significantly larger ($P < .05$ compared with the control group), but there was no improvement in the failure load or the ultimate strength of the PPT (both $P > .05$); only the stiffness was shown to increase significantly ($P < .05$, compared with the control group). No significant differences were seen in the failure load, ultimate strength, or stiffness between the CGRP-antagonist group and the control group ($P > .05$ for all). At postoperative week 16, the CSA values for all 3 groups were reasonably similar ($P > .05$), but the failure load, ultimate strength, and stiffness values were significantly higher in the CGRP group ($P < .05$) and lower in the CGRP-antagonist group ($P < .01$) compared with the control group. When we compared the CGRP and CGRP-antagonist groups, we were able to show that blocking the CGRP receptors significantly reduced failure load, ultimate strength, and stiffness at weeks 8 and 16 postoperatively ($P < .05$ for all).

It is disappointing that all 3 groups retained the rupture around the osteotomy site between the newly formed bone and the proximal patella; nonetheless, based on our analyses, the results at 16 weeks postoperatively (Table 2) had a <5% chance of being incorrect.

DISCUSSION

The data in this study indicated that when CGRP was locally delivered to the bone-tendon healing interface of a rabbit partial patellectomy model early in the healing process, the degree of osteogenesis was increased, and the mechanical properties were improved compared with the control group at week 16. In contrast, when the CGRP receptors were antagonized by the introduction of BIBN4096BS around the BTI, the degree of bone mineralization decreased, and the mechanical properties decreased. These observations seem to support the hypothesis that CGRP promotes healing of the BTI by enhancing osteogenesis. In addition, sensory neurotransmitters are widely distributed in the paratenon; therefore, this study suggests that normal paratenons should be protected as far as possible during the reconstruction process, especially in tendon-related injuries such as rotator cuff repair, patellar tendon repair, and Achilles tendon repair, in an effort to enhance the healing of the BTI.

New bone formation has been shown to be the foundation of functional recovery after BTI injury.[17,19] In the current study, we noted an increase in new bone production from the original osteotomy site of the remaining patella in the CGRP group (including new bone area, BMD, and relative BMC), but there was less new bone formation in the CGRP-antagonist group compared with the control group. The particularly high values of BMD in the CGRP group at 8 weeks were the most obvious demonstration of accelerated osteogenesis in the CGRP group. The decrease in these values at 16 weeks is explained by the formation of mature marrow cavities.[10]

The extremely low BMD values in the CGRP-antagonist group evidenced the effect of inhibiting CGRP activity. The histologic findings also showed more newly formed trabecular bone in the CGRP group, and at 16 weeks postoperatively, the morphology of this newly formed bone was more similar to that of the residual patella. In addition, fewer bone mass and a higher number of large marrow cavities were seen in the CGRP-antagonist group. MLRS analysis confirmed the osteogenic effects of CGRP described in this study. MLRS has been proven especially useful for evaluating osteogenesis and other bone disorders[20] because it can provide information about bone mineral and matrix composition, which are related to the bone's mechanical properties and health.[25]

In this study, we analyzed only the relative BMC (peak at 960 cm^{-1}) of the new bone compared with the residual patella, and we demonstrated that this value increased in all 3 groups over time, reaching nearly 85% of the residual patellar BMC in the control group after 16 weeks. It is worth noting that the BMC value for the CGRP-antagonist group reached only 65% of this value and the BMC value of the CGRP group exceeded 100%, but these findings could not indicate whether the new bone in the CGRP group was perfect or normal. The failure load of these specimens in previous reports was nearly 65% of that of the normal PPT complexes,[19,33] which may be associated with bone loss in the remaining proximal patella after surgery and immobilization.

Although the area, BMD, and relative BMC of the newly formed bone in the CGRP group were significantly higher than were the values in the control group at 8 weeks postoperatively, there was no significant improvement in the failure load or ultimate strength of these PPT complexes. This suggests that newly formed bone is just 1 index for BTI healing and that advanced remodeling might play a vital role in physiologic function.[19] The histologic results showed that the CGRP group had more trabecular bone around the interface of the proximal patella and patellar tendon at 8 weeks; however, no more mature trabecular pattern formations, characterized by a lack of well-developed lamellae and marrow cavities, were observed. When the CGRP receptors were antagonized, osteogenesis was very slow, and there was little new bone formation at week 8; however, the biomechanical properties of these PPT complexes were not significantly lower than were those of the control group. Although the in-growth of new nerve fibers containing CGRP might be a prerequisite for fracture healing and remodeling,[15] the results in this study indicated that increased local CGRP at the early stages of BTI healing was able to accelerate osteogenesis but did not facilitate bone remodeling.

During the healing process of BTI injuries, the initiation event is usually endochondral ossification,[33] which is often seen in fracture healing.[27] Similar to the healing of bone fractures, BTI healing involves osteoblasts, osteoclasts, and mesenchymal stem cells.[14,28] Years of research have demonstrated that CGRP receptors are present on all of these cells,[30,31] which may explain its effect on osteogenesis. As for osteoblasts, CGRP showed a positive effect on osteoblast proliferation and differentiation and was able to reduce osteoblast apoptosis in inflammatory conditions.[37] Targeted overexpression of CGRP in osteoblasts enhanced

bone density in mice, whereas mice lacking α-CGRP showed reduced bone formation and osteopenia.[26] In a rabbit bone defect model, inhibition of osteoclastic bone resorption activity was shown to occur after CGRP receptor binding.[4] In vitro, CGRP may regulate bone metabolism by inhibiting osteoclast formation,[8] whereas studies have shown that CGRP can promote bone mesenchymal stem cell osteogenic differentiation and osteogenic ability linked to the higher expression of osteogenesis-related indexes alkaline phosphatase, bone sialoprotein, and runt-related transcription factor 2.[13,35] Recombinant human CGRP can induce rabbit adipose-derived stem cells into osteoblast differentiation.[11]

This study has several limitations. First, the biomechanical properties of rabbit and human knee differ notably, and thus it is not appropriate to simply translate these results to humans. However, the rabbit PPT complex is still a good model to study the BTI healing process. Second, we did not analyze the regeneration of the fibrocartilage zone, which is also very important for the repair quality of BTI. Although the H&E staining results showed that fibrocartilage zone regeneration was improved in the CGRP group and was inhibited in the CGRP-antagonist group, we focused only on the osteogenic properties of these compounds in this study. Third, the relative BMC (detected using MLRS) used here to measure the mineralization of new bone was not perfect, but it was able to reflect the change of new bone mineralization to some extent. More animal studies with larger sample sizes are needed before clinical trials can be designed and completed.

CONCLUSION

This study demonstrated that locally administering exogenous CGRP at the early stages of BTI healing may enhance osteogenesis in a rabbit partial patellectomy model, ultimately leading to a better quality of bone-tendon repair. However, exogenous CGRP did not facilitate bone remodeling. Although CGRP is known to affect vascular dilation in the clinic, this study may help to build a scientific foundation for future clinical therapies for BTI injuries.

REFERENCES

1. Ackermann PW, Franklin SL, Dean BJ, et al. Neuronal pathways in tendon healing and tendinopathy—update. *Front Biosci (Landmark Ed)*. 2014;19:1251-1278.
2. Agout C, Berhouet J, Bouju Y, et al. Clinical and anatomic results of rotator cuff repair at 10 years depend on tear type. *Knee Surg Sports Traumatol Arthrosc*. 2018;26(8):2490-2497.
3. Cadosch D, Gautschi OP, Thyer M, et al. Humoral factors enhance fracture-healing and callus formation in patients with traumatic brain injury. *J Bone Joint Surg Am*. 2009;91(2):282-288.
4. Chen J, Liu W, Zhao J, et al. Gelatin microspheres containing calcitonin gene-related peptide or substance P repair bone defects in osteoporotic rabbits. *Biotechnol Lett*. 2017;39(3):465-472.
5. Danielson P, Alfredson H, Forsgren S. Distribution of general (PGP 9.5) and sensory (substance P/CGRP) innervations in the human patellar tendon. *Knee Surg Sports Traumatol Arthrosc*. 2006;14(2):125-132.
6. Deprés-Tremblay G, Chevrier A, Snow M, et al. Rotator cuff repair: a review of surgical techniques, animal models, and new technologies under development. *J Shoulder Elbow Surg*. 2016;25(12):2078-2085.
7. Grässel SG. The role of peripheral nerve fibers and their neurotransmitters in cartilage and bone physiology and pathophysiology. *Arthritis Res Ther*. 2014;16(6):485.
8. He H, Chai J, Zhang S, et al. CGRP may regulate bone metabolism through stimulating osteoblast differentiation and inhibiting osteoclast formation. *Mol Med Rep*. 2016;13(5):3977-3984.
9. Hu J, Qu J, Xu D, et al. Combined application of low-intensity pulsed ultrasound and functional electrical stimulation accelerates bone-tendon junction healing in a rabbit model. *J Orthop Res*. 2014;32(2):204-209.
10. Hu J, Zhang T, Xu D, et al. Combined magnetic fields accelerate bone-tendon junction injury healing through osteogenesis. *Scand J Med Sci Sports*. 2015;25(3):398-405.
11. Huang CZ, Yang XN, Liu DC, Sun YG, Dai XM. Calcitonin gene-related peptide-induced calcium alginate gel combined with adipose-derived stem cells differentiating to osteoblasts. *Cell Biochem Biophys*. 2015;73(3):609-617.
12. Irie K, Hara-Irie F, Ozawa H, Yajima T. Calcitonin gene-related peptide (CGRP)-containing nerve fibers in bone tissue and their involvement in bone remodeling. *Microsc Res Tech*. 2002;58(2):85-90.
13. Jia S, Zhang SJ, Wang XD, et al. Calcitonin gene-related peptide enhances osteogenic differentiation and recruitment of bone marrow mesenchymal stem cells in rats. *Exp Ther Med*. 2019;18(2):1039-1046.
14. Kawakami Y, Takayama K, Matsumoto T, et al. Anterior cruciate ligament-derived stem cells transduced with BMP2 accelerate graft-bone integration after ACL reconstruction. *Am J Sports Med*. 2017;45(3):584-597.
15. Li J, Kreicbergs A, Bergström J, Stark A, Ahmed M. Site-specific CGRP innervation coincides with bone formation during fracture healing and modeling: a study in rat angulated tibia. *J Orthop Res*. 2007;25(9):1204-1212.
16. Li Y, Tan Y, Zhang G, Yang B, Zhang J. Effects of calcitonin gene-related peptide on the expression and activity of nitric oxide synthase during mandibular bone healing in rabbits: an experimental study. *J Oral Maxillofac Surg*. 2009;67(2):273-279.
17. Lu H, Hu J, Qin L, et al. Area, length and mineralization content of new bone at bone-tendon junction predict its repair quality. *J Orthop Res*. 2011;29(5):672-677.
18. Lu H, Qin L, Cheung W, et al. Low-intensity pulsed ultrasound accelerated bone-tendon junction healing through regulation of vascular endothelial growth factor expression and cartilage formation. *Ultrasound Med Biol*. 2008;34(8):1248-1260.
19. Lu H, Qin L, Fok P, et al. Low-intensity pulsed ultrasound accelerates bone-tendon junction healing: a partial patellectomy model in rabbits. *Am J Sports Med*. 2006;34(8):1287-1296.
20. Matousek P, Stone N. Development of deep subsurface Raman spectroscopy for medical diagnosis and disease monitoring. *Chem Soc Rev*. 2016;45(7):1794-1802.
21. Mishima H, Sugaya H, Yoshioka T, et al. The effect of combined therapy, percutaneous autologous concentrated bone marrow grafting and low-intensity pulsed ultrasound (LIPUS), on the treatment of non-unions. *J Orthop Trauma*. 2016;30(8):S2.
22. Morris MD, Mandair GS. Raman assessment of bone quality. *Clin Orthop Relat Res*. 2011;469(8):2160-2169.
23. Niedźwiedzki T, Filipowska J. Bone remodeling in the context of cellular and systemic regulation: the role of osteocytes and the nervous system. *J Mol Endocrinol*. 2015;55(2):R23-R36.
24. O'Brien R, Muller K. *Applied Analysis of Variance in Behavioral Science*. Marcel Dekker; 1993.
25. Peterson JR, Okagbare PI, De La Rosa S, et al. Early detection of burn induced heterotopic ossification using transcutaneous Raman spectroscopy. *Bone*. 2013;54(1):28-34.
26. Schinke T, Liese S, Priemel M, et al. Decreased bone formation and osteopenia in mice lacking alpha-calcitonin gene-related peptide. *J Bone Miner Res*. 2004;19(12):2049-2056.

27. Schlundt C, El Khassawna T, Serra A, et al. Macrophages in bone fracture healing: their essential role in endochondral ossification. *Bone*. 2018;106:78-89.
28. Struewer J, Roessler PP, Schuettler KF, et al. Influence of cyclical mechanical loading on osteogenic markers in an osteoblast-fibroblast co-culture in vitro: tendon-to-bone interface in anterior cruciate ligament reconstruction. *Int Orthop*. 2014;38(5):1083-1089.
29. Tuzmen C, Verdelis K, Weiss L, Campbell P. Crosstalk between substance P and calcitonin gene-related peptide during heterotopic ossification in murine Achilles tendon. *J Orthop Res*. 2018;36(5):1444-1455.
30. Villa I, Mrak E, Rubinacci A, Ravasi F, Guidobono F. CGRP inhibits osteoprotegerin production in human osteoblast-like cells via cAMP/PKA-dependent pathway. *Am J Physiol Cell Physiol*. 2006;291(3):C529-C537.
31. Wang L, Shi X, Zhao R, et al. Calcitonin-gene-related peptide stimulates stromal cell osteogenic differentiation and inhibits RANKL induced NF-kappaB activation, osteoclastogenesis and bone resorption. *Bone*. 2010;46(5):1369-1379.
32. Wang XY, Guo X, Qu SX, Weng J, Cheng CY. Temporal and spatial CGRP innervation in recombinant human bone morphogenetic protein induced spinal fusion in rabbits. *Spine (Phila Pa 1976)*. 2009;34(22):2363-2368.
33. Xu D, Zhang T, Qu J, Hu J, Lu H. Enhanced patella—patellartendon healing using combined magnetic fields in a rabbit model. *Am J Sports Med*. 2014;42(10):2495-2501.
34. Yamaguchi T, Ochiai N, Sasaki Y, et al. Efficacy of hyaluronic acid or steroid injections for the treatment of a rat model of rotator cuff injury. *J Orthop Res*. 2015;33(12):1861-1867.
35. Yu X, Liu S, Chen H, et al. CGRP gene-modified rBMSCs show better osteogenic differentiation capacity in vitro. *J Mol Histol*. 2018;49(4):357-367.
36. Zhang Y, Xu J, Ruan YC, et al. Implant-derived magnesium induces local neuronal production of CGRP to improve bone-fracture healing in rats. *Nat Med*. 2016;22(10):1160-1169.
37. Zhou Y, Zhang H, Zhang G, et al. Calcitonin gene-related peptide reduces *Porphyromonas gingivalis* LPS-induced TNF-α release and apoptosis in osteoblasts. *Mol Med Rep*. 2018;17(2):3246-3254.

APPENDIX

In Vitro Drug Release and Sustainability Analysis

To evaluate the rate of calcitonin gene-related peptide (CGRP) and CGRP receptor antagonist (BIBN4096BS) release from the fibrin sealant, which contained 200 μL of fibrinogen, 40 μL of thrombin, and 6.0 mg of CGRP or 1.5 mg of BIBN4096BS, we incubated each gel in 0.5 mL of phosphate-buffered saline supplemented with 10% fetal bovine serum (PBS-FBS solution) at 37°C with continuous rotation using a microhybridization incubator for 14 days. The PBS-FBS solution was replaced and collected 5 times over the first 24 hours and then changed and collected daily until day 14. These wash solutions were then subjected to enzyme-linked immunosorbent assay for CGRP and BIBN4096BS, and the release experiment was carried out 3 times. The cumulative percentages are presented in Appendix Table A1 and show that a mean ± SD of 26.4% ± 2.6% of the total CGRP and 31.2% ± 3.7% of the total BIBN4096BS in the fibrin sealant were released into the PBS-FBS solution at 24 hours and that >50% of the total CGRP and BIBN4096BS were released into the wash solution by 72 hours. On day 14 of the experiment, 98.2% ± 4.4% of the total CGRP and 98.8% ± 5.4% of the total BIBN4096BS had been released from these gels.

TABLE A1
In Vitro Drug Release and Sustainability Analysis[a]

Time, d	Release Rate, %		
	Control	CGRP	CGRP Receptor Antagonist
1	0	26.4 ± 2.6	31.2 ± 3.7
2	0	41.3 ± 3.3	48.5 ± 4.5
3	0	53.6 ± 4.4	61.3 ± 4.8
4	0	62.5 ± 4.7	72.1 ± 5.4
5	0	71.4 ± 4.5	80.4 ± 5.6
6	0	78.3 ± 4.6	85.1 ± 5.6
7	0	84.6 ± 4.6	89.6 ± 5.4
8	0	89.3 ± 4.3	92.8 ± 5.3
9	0	93.6 ± 4.5	94.4 ± 5.6
10	0	95.2 ± 4.6	96.7 ± 5.5
11	0	96.5 ± 4.3	97.3 ± 5.3
12	0	97.1 ± 4.5	98.1 ± 5.4
13	0	97.8 ± 4.4	98.5 ± 5.6
14	0	98.2 ± 4.4	98.8 ± 5.4

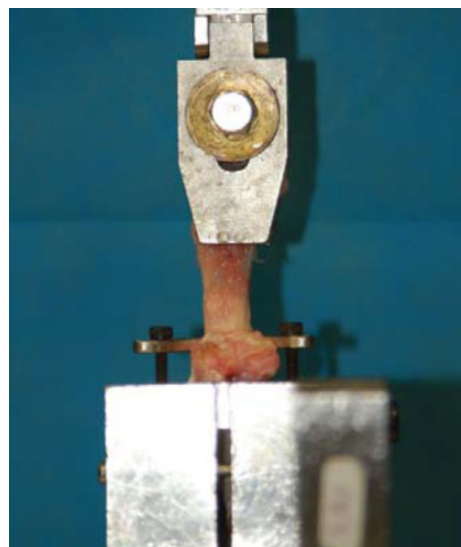[a]Data are reported as mean ± SD. CGRP, calcitonin gene-related peptide.

Figure A1. Mechanical testing of the patella–patellar tendon complex using a custom-made jig that includes an upper clamp and a lower clamp to fix the patella and the proximal tibia, respectively.